*Int. J. Electrochem. Sci.*, 10 **(2015)** 10307 - 10320

International Journal of
ELECTROCHEMICAL
SCIENCE
www.electrochemsci.org

# Effect of Compression on Negative Lead-Acid Battery Electrodes Doped with Glass Fibres

*P. Bača*[*], *P. Křivík, J. Zimáková, D. Fryda*

Faculty of Electrical Engineering and Communication, Brno University of Technology, 61600 Brno, Czech Republic
[*]E-mail: baca@feec.vutbr.cz

*Received:* 23 June 2015 / *Accepted:* 19 September 2015 / *Published:* 4 November 2015

Lead-acid battery with negative electrodes doped with microscopic glass fibres are comparable with those doped with carbon or titanium dioxide during accelerated PSoC cycling and reach a long cycle life. The performance of these electrodes can be even elevated by applying moderate compression of 4 $N.cm^{-2}$.

**Keywords:** lead-acid battery electrodes, glass fibres, mechanical compression

## 1. INTRODUCTION

Degradation mechanism of lead-acid batteries during standing in the partial state of charge (PSoC) for a long time is sulphation of negative active mass [4]. This phenomenon can be found especially in hybrid electric vehicles (HEV). Lead sulphate formed during discharge undergoes recrystallization of originally fine crystals. These crystals become larger. VRLA battery loses capacity by this mechanism and part of the current during charge is consumed by the oxygen cycle. Oxygen evolved during charging at the positive electrode travels to the negative electrode where is reduced to water [1,2].

This problem was solved by many researchers. The application of pulse current during charging could minimize the “hard sulphate” formation [3,19]. Another approach is small addition of certain types of carbon to the negative paste which leads to the hindrance of sulphation [5,6]. Team of researchers sponsored by ALABC [7] found that addition of about 2% of carbon black or powdered graphite to the negative active mass paste indeed hinders the negative electrode sulphation.

The mechanism of this effect is not clear. Nakamura et al. [5] tested standard VRLA battery cells and found 20% of lead sulphate in positive plates and 40% in the negative plates after 400 of simulation cycles. While lead sulphate on the positive plates could be recharged, lead sulphate on the negative plates showed 20% of sulphate after recharging. When was increased the carbon content in the negative active mass paste ten times, the cells undergoes 1100 of simulation cycles and the sulphate content in the negative active mass was 30%, and only 10% after recharging. Standard content of carbon black in the negative mass is about 0.2% [8]. Another authors [5,6] found the positive effect of carbon in the creation of conducting bridges from the particles of carbon surrounding the lead sulphate crystals. It was demonstrated by SEM microphotographs. Some authors [7] investigated that the addition of carbon to the negative mass in the unformed state increased its conductivity. They supposed that the same effect takes place in the negative active mass after formation if the negative electrode is highly sulphated. We measured the resistance of the negative active mass both in the charged and discharged state during mechanical pressures and also during cycling [9]. The resistance of the negative active mass between two neighbouring electrode ribs was found between 0.2 and 0.5 mΩ. The difference between the values of resistances in the charged and discharged state was minimal. The resistance of the positive active mass was 7–8 mΩ in the charged state and 20–50 mΩ in the discharged state. That is why the attempt to improve the conductivity of the negative mass by the carbon addition, that is less conductor than lead, has no sense. Carbon can be also used for positive plates of lead-acid battery (CLAB), where porous carbon grids coated with lead was tested in [20].

Chemical process in lead-acid batteries during discharge and charge was discussed with help of mechanism of the dissolution–precipitation [10–12]. This process is possible during discharge, where was formed supersaturated solution of sulphate, followed by nucleation and crystallization of lead sulphate. But the charging process requires sulphate solubility about $10^{-5}$ molar [10] and in the electrolyte this value is an order of magnitude lower. That is why it seems that the reaction site is the contact between lead sulphate and the current collector [12] and diffusion transport has low importance. The efficiency of this charging process is low when the crystals of lead sulphate are larger than a few μm. In positive active mass this is no problem because their pores in the charged state are very little from 0.05 to 2 μm [13,14], and that is why the sulphate crystals are limited in their size [13]. The pores of negative electrodes are larger. Their specific BET surface area is 0.5–0.8 $m^2\ g^{-1}$ [15] when compared with the positive electrodes with 6.4 $m^2\ g^{-1}$ [13]. This means that crystals of the lead sulphate have much more space for their growth in negative active mass pores when the battery is without current charge or in the PSoC regime. When adding the finely powdered graphite into the negative active mass, the pores will be occupied by the graphite particles and size of crystals of the lead sulphate will be limited. If this theory is correct, the graphite does not improve electric conductivity of negative active mass, and we can use even nonconducting additives [4].

In our work [16], we focused on the limitation of the irreversible sulphation of negative active mass of explored electrodes in the course of PSoC cycling. The negative active mass was doped with two additives – carbon and titanium dioxide as a nonconducting powder. Electrodes were subjected to a defined pressure. Accelerated cycling showed that electrodes doped with carbon perform better than those doped with $TiO_2$ and mechanical pressure of 4 N $cm^{-2}$ has a positive effect on the cycle life of negative electrodes.

Analogous experiments were performed in this work with other non-conductive additives in negative active mass, such as glass fibres. These additives along with optimal compression could limit the irreversible sulphation of negative electrodes during PSoC cycling. Experiments to support this conclusion form the subject of the present work.

## 2. EXPERIMENTAL SECTION

### *2.1. Preparation of cells and formation*

The negative electrodes with dimensions of 55 × 20 × 7 mm were equipped with system of parallel, insulated ribs, pasted with an active material without any form of carbon but doped with glass fibres provided by Hollingworth and Vose Comp. These glass fibres were on the average 10 – 35 μm in length and up to nearly 2 μm in thickness. Their appearance was a white powder. The concentration of glass fibres in the active mass was 2.65 mass percent which has shown good properties in the preceding experiments [17]. The electrodes were then placed in cells with two counter electrodes and with the electrolyte of 1.28 g $cm^{-3}$ density and with AGM separators of the type BG260 EB170 (1.7 mm in thickness).

The cells were subjected to 24 formation cycles (4 h charging and 2 h stand) lasting for 144 h in total.

### *2.2. Conditioning cycles – first run*

The conditioning cycles in the flooded state consisted of 0.7 A discharge current up to a voltage of 1.6 V followed by charging with the same current up to 2.45 V cut-off, the whole cycle taking 24 hours. During conditioning cycles capacities of all cells were measured.

### *2.3. Accelerated PSoC cycling – first run*

Prior to the first PSoC run, the surplus electrolyte in the cells was sucked off, the cells were hermetized, the desired pressure on the electrodes was applied (three electrodes were subject to a compression of 2, 4, and 6 $N.cm^{-2}$ respectively). The equipment produced a defined pressure on the active electrode surface by means of a thrust screw is described in [16]. The pressure was measured by using tensometric sensors. After application of compression on the electrodes, they were discharged to 50% of the measured capacity. The pressure was checked every two days to keep the desired value. PSoC run contained the following four steps:

25 s of charging with a current of 2.5 A, 3 s of standing, 25 s of discharging with a current of 2.495 A and 3 s of standing. As soon as the cell voltage dropped below 1.5 V, the measurement was finished.

In total, over 62,000 cycles were applied for all three PSoC runs (20,000, 28,000, and 14,000). During all three PSoC runs were measured contact resistance and active mass resistance of the negative electrodes. The conditioning cycles and the capacity were determined after each run.

### *2.4. Conditioning cycles – second run*

After finishing the first PSoC run, the experimental cells were in the hermetic state due to two conditioning cycles with the same parameters as after formation. During conditioning cycles capacities of all cells were measured.

### *2.5. PSoC cycling – second run*

All of parameters are analogous to the preceding case. The voltage and potentials of the negative electrodes were again measured at the end of charge or discharge at every hundredth cycle.

### *2.6. Conditioning cycles – third run*

After finishing the second PSoC run, the experimental cells were in the hermetic state due to two conditioning cycles with the same parameters as after formation. During conditioning cycles capacities of all cells were measured.

### *2.7. PSoC cycling – third run*

All of parameters are analogous to the preceding case. The voltage and potentials of the negative electrodes were again measured at the end of charge or discharge at every hundredth cycle.

## 3. RESULTS AND DISCUSSION

### *3.1. Conditioning cycles – first run*

In Fig. 1 is shown the course of the capacities with the number of conditioning cycles. It can be seen that the capacities of all three cells rise slowly during 15 conditioning cycles from about 2.4 Ah up to about 3 Ah.

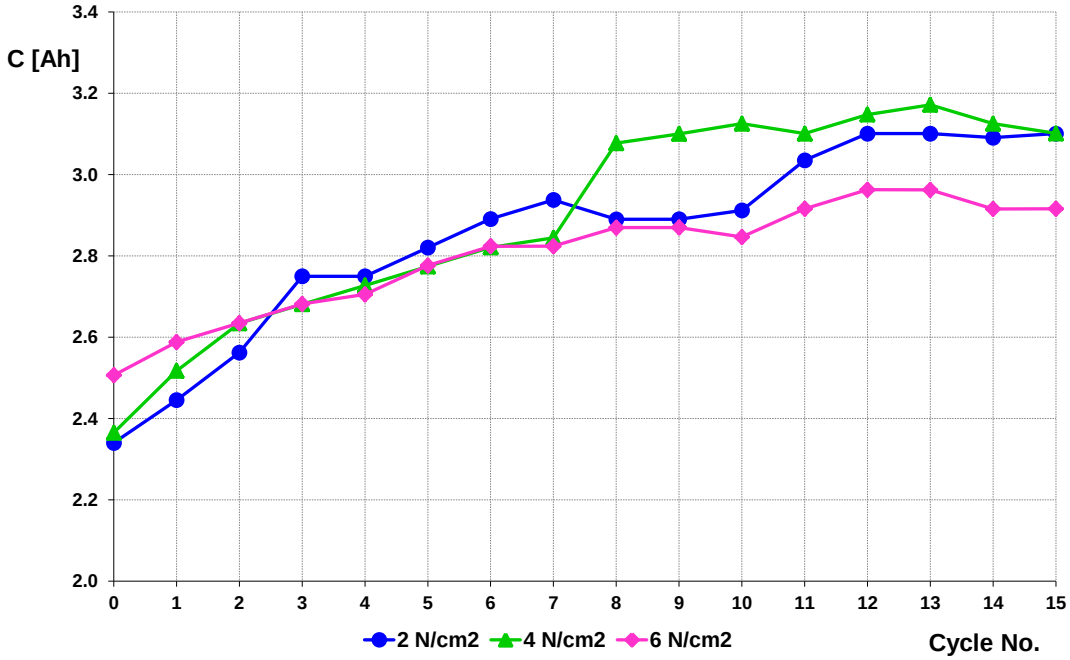


**Figure 1.** Dependence of the cell capacities on the number of conditioning cycles

### *3.2. Accelerated PSoC cycling – first run*

#### *3.2.1. Charging half-cycles*

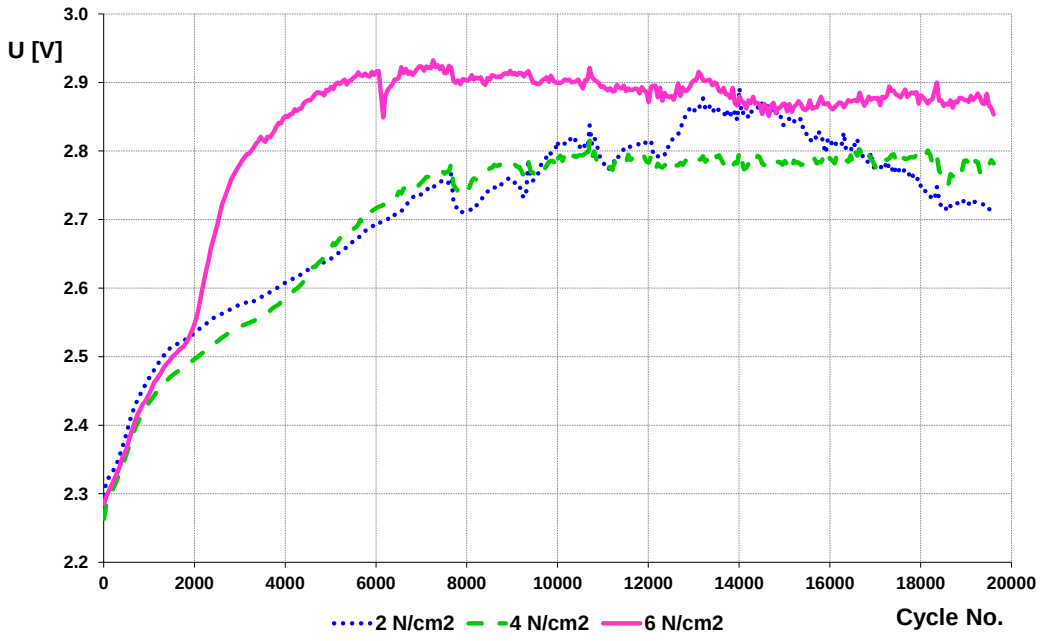


**Figure 2.** Dependence of cell voltage on the number of charging half-cycles

The cell voltages measured at the end of charging half-cycles after every hundredth of the PSoC cycle can be seen on Fig. 2. The changes of the cell voltages are due to the negative electrodes. The conspicuous break in the charging characteristics of cell with pressure of 6 N.cm$^{-2}$ with steep raise toward higher values of voltages is related with the start of hydrogen evolution. Nevertheless, raise of voltage of the cell with 2 and 4 N.cm$^{-2}$ is not so steep, perhaps due to a more intense oxygen cycle. Oxygen cycle of the cell with pressure of 6 N.cm$^{-2}$ was suppressed probably due to excessive compression of the separator.

### *3.2.2. Discharging half-cycles*

The cell voltages measured at the end of discharging half-cycles after every hundredth of the PSoC cycle can be seen on Fig. 3.

The cell with pressure of 2 N.cm$^{-2}$ has the biggest drop of voltage due to high internal resistance of the cell.

Inside the cell with pressure of 6 N.cm$^{-2}$ large compression apparently caused a reduction in porosity of the active mass and separator, voltage decreases as at the cell with pressure of 2 N.cm$^{-2}$. This cell has a higher internal resistance than the cell with pressure of 4 N.cm$^{-2}$, although not as high as the cell with pressure of 2 N.cm$^{-2}$ - see Figs. 11 to 12. At the end PSoC run, the voltage drop of the cell with pressure of 6 N.cm$^{-2}$ is stopped. Here, a higher pressure has a positive effect on the cell. The value of internal resistance is reduced, the structure of the negative active mass become stabilized and the charge efficiency increases.

The least drop in the voltage was observed by the cell with pressure of 4 N.cm$^{-2}$. That pressure is sufficient to stabilize the structure of the negative active mass and to reduce the internal resistance of the cell. However porosity of negative active mass and separator remains at high level.

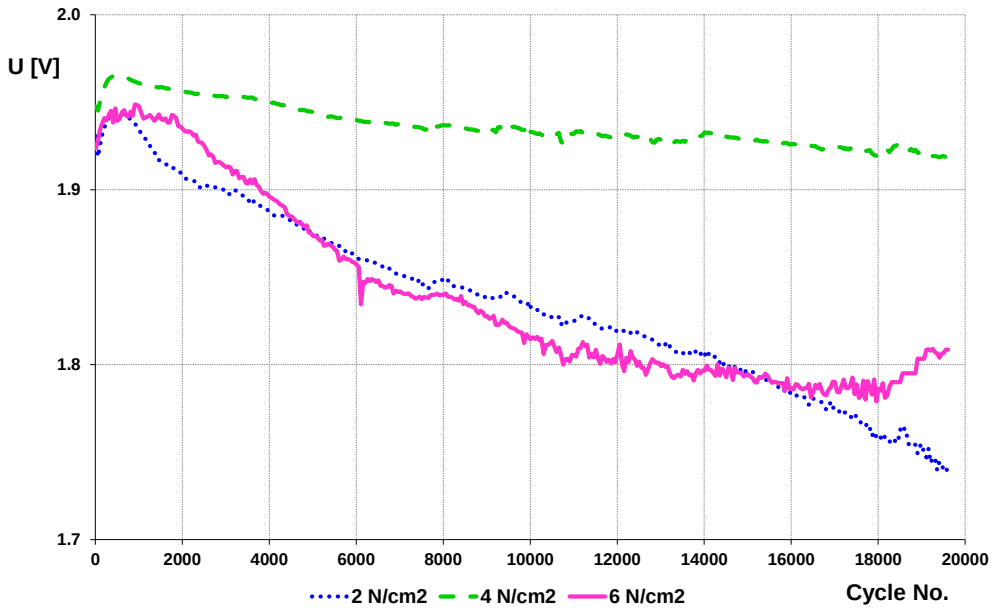


**Figure 3.** Dependence of cell voltage on the number of discharging half cycles

*3.2.3. Mechanical pressure changes*

Courses of the mechanical pressure in the 1st PSoC run can be seen on Fig. 4.

From course of characteristics, we can see a step changes, caused by manual adjusting of compression. At the beginning of PSoC run the pressure changes are accompanied by a large drop, which is most pronounced at the cell with the highest applied pressure (6 $N.cm^{-2}$), by about 2 $N.cm^{-2}$. For the cell with the applied pressure 4 $N.cm^{-2}$, this drop is about 1 $N.cm^{-2}$. We assume that this phenomenon is caused by the fact, that at the higher compression of the cells, AGM separators are compressed and partially absorb the pressure, and thus decreases their thickness. This phenomenon for the cell with the applied pressure 2 $N.cm^{-2}$ is less noticeable because the pressure on the electrode system is small. Low pressure does not lead to stabilization of the structure of the active mass, that can gradually expands during cycling.

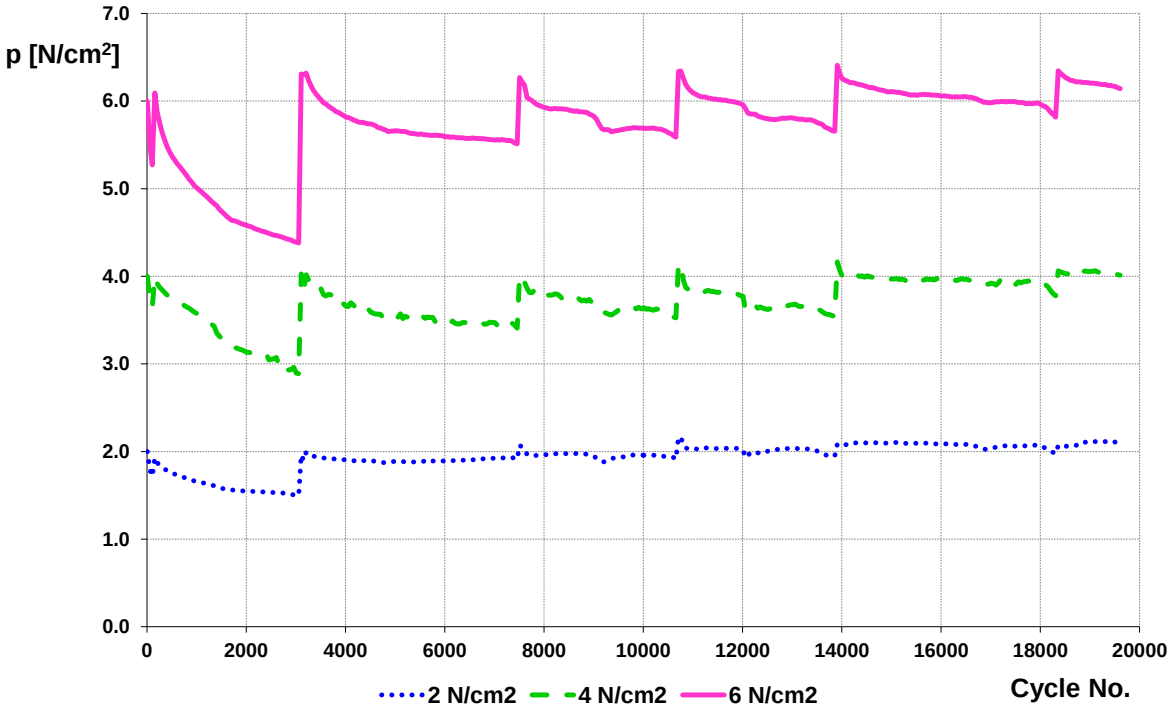


**Figure 4.** Course of the mechanical pressure in the 1st PSoC run

*3.3. PSoC cycling – second run*

*3.3.1. Charging half-cycles*

The charging characteristic of the second run is shown in Fig. 5. The lower voltage compared to the first run may be attributed to the circumstances that the internal oxygen cycle is apparently running from the start of PSoC cycling. The maximum values of the charging voltage did not surpass 2.6 V.

The tips appearing on charging characteristics are caused by adjusting of desired pressure on the electrode system. That adjusting always causes temporary increase of voltage. This phenomenon is probably caused by suppression of oxygen cycle due to the temporary filling of the separator free pores by the electrolyte during pressure adjusting.

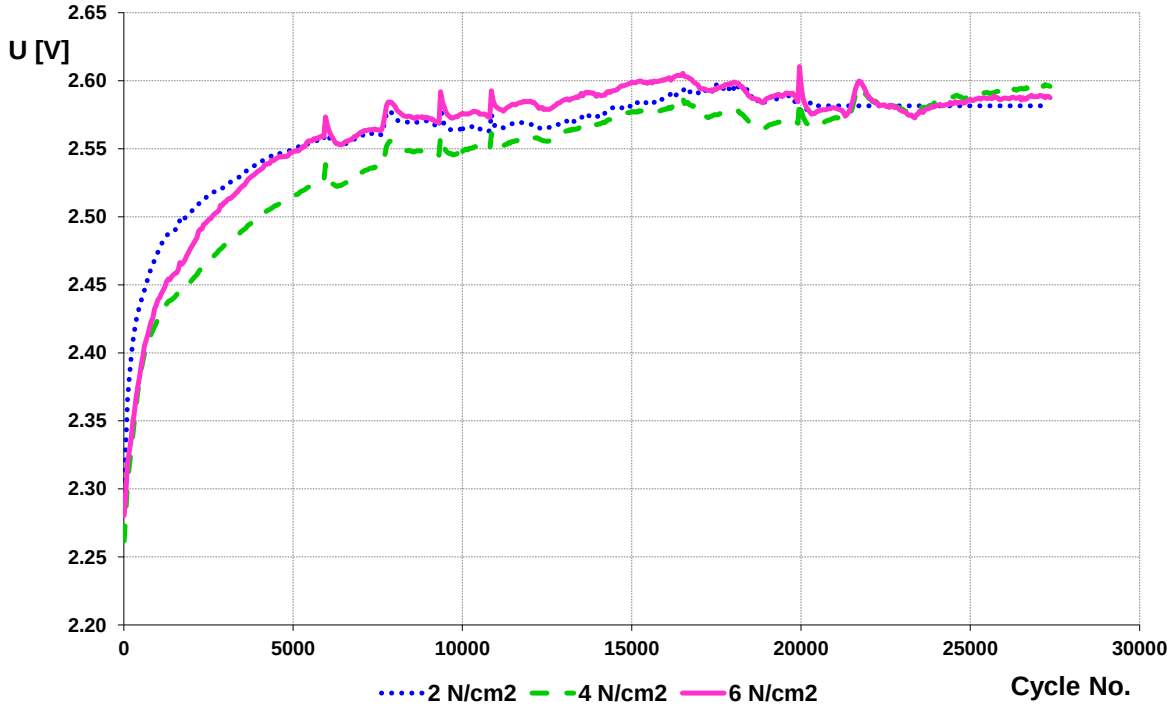


**Figure 5.** Dependence of the cell voltage on the number of charge half-cycles

*3.3.2. Discharging half-cycles*

The discharge characteristics are shown in Fig. 6. It can be seen that with the electrodes operating at higher compression the voltage during discharge decreases only very little or it is in good condition and it attains high charge acceptance. A more expressed voltage drop is observed with cell with lowest compression which collapsed after 18,000 cycles. This is probably related to the high internal resistance and poor charge acceptance during charging caused by low pressure applied on the active mass of the negative electrode.

When comparing the second PSoC run with the preceding experiment, it is obvious that the final voltage attained after 27,000 cycles is higher and the cells with defined compression have (except for the cell with lowest compression) higher performance and longer life time.

At the cell with pressure of 4 $N.cm^{-2}$ occurs during PSoC cycling even a slight increase in voltage. Most likely this is due to the very good charge acceptance during charging. Because the charging current is 2.5 A and discharging current is 2.495 A, the cell obtains during charging about 0.2% more of charge than returns during discharging.

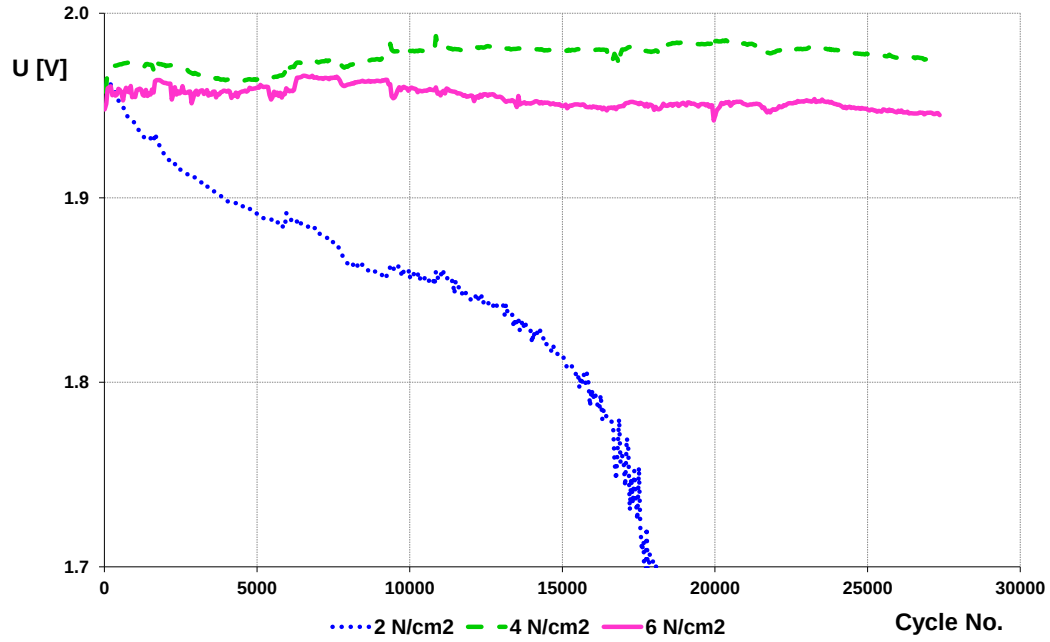


**Figure 6.** Dependence of cell voltage on the cycle number. Second PSoC run

*3.4. PSoC cycling – third run*

*3.4.1. Charging half-cycles*

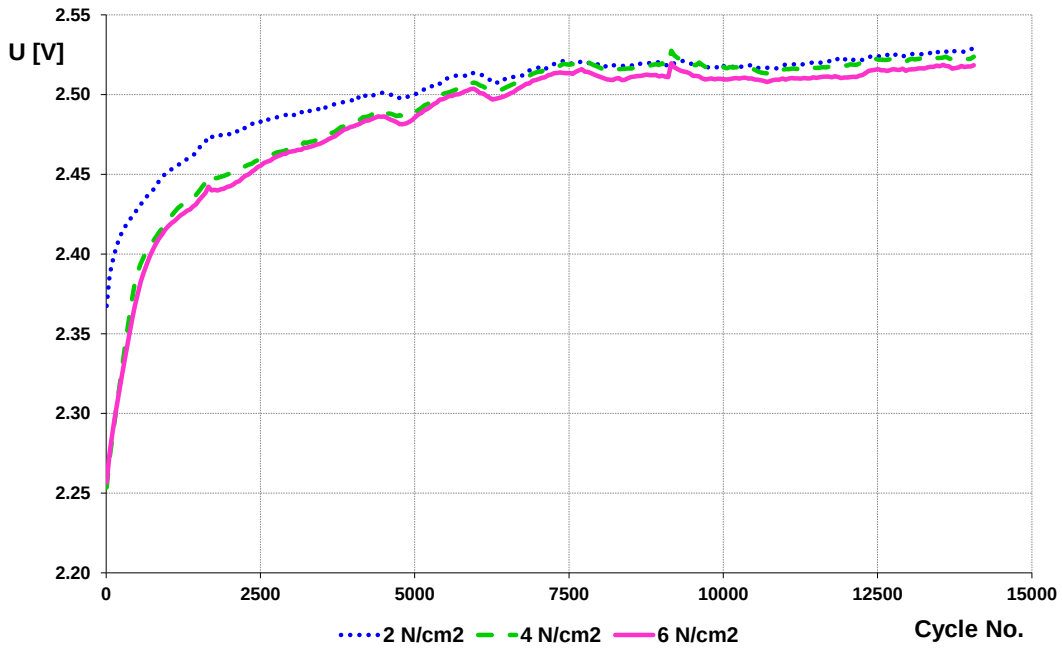


**Figure 7.** Dependence of cell voltage on charging cycle number. Third PSoC run

The last PSoC run, which took place after the third conditioning cycling, included 14,000 PSoC cycles; their course is depicted in Fig. 7. The charging characteristics show a moderate growth of the voltage with a subsequent steady state at 2.55 V.

Again, this is due to the fact that it was launched internal oxygen cycle inside cells. Highest voltage at the beginning of PSoC cycling was at the cell with the lowest compression due to high internal resistance.

### *3.4.2. Discharging half-cycles*

The corresponding discharge characteristics are illustrated in Fig. 8. Electrode with compression of 2 N.cm$^{-2}$ shows again a voltage decrease, although less steep, during discharge.

The course of the voltage at the electrode is similar to the previous PSoC run, except that the third PSoC run was interrupted earlier, already after 14,000 of PSoC cycles. Therefore voltage did not drops below 1.7 V as in the 2nd PSoC run, which lasted for 28,000 of PSoC cycles and the cell with the lowest pressure collapsed after 18,000 of PSoC cycles.

For the cell with pressure of 4 N.cm$^{-2}$ occurs during PSoC cycling again a slight increase in voltage (from 1.97 V to 1.99 V), due to a very good charge acceptance during charging.

For the cell with pressure of 6 N.cm$^{-2}$ the voltage is almost constant during PSoC cycling and its value is around 1.98 V.

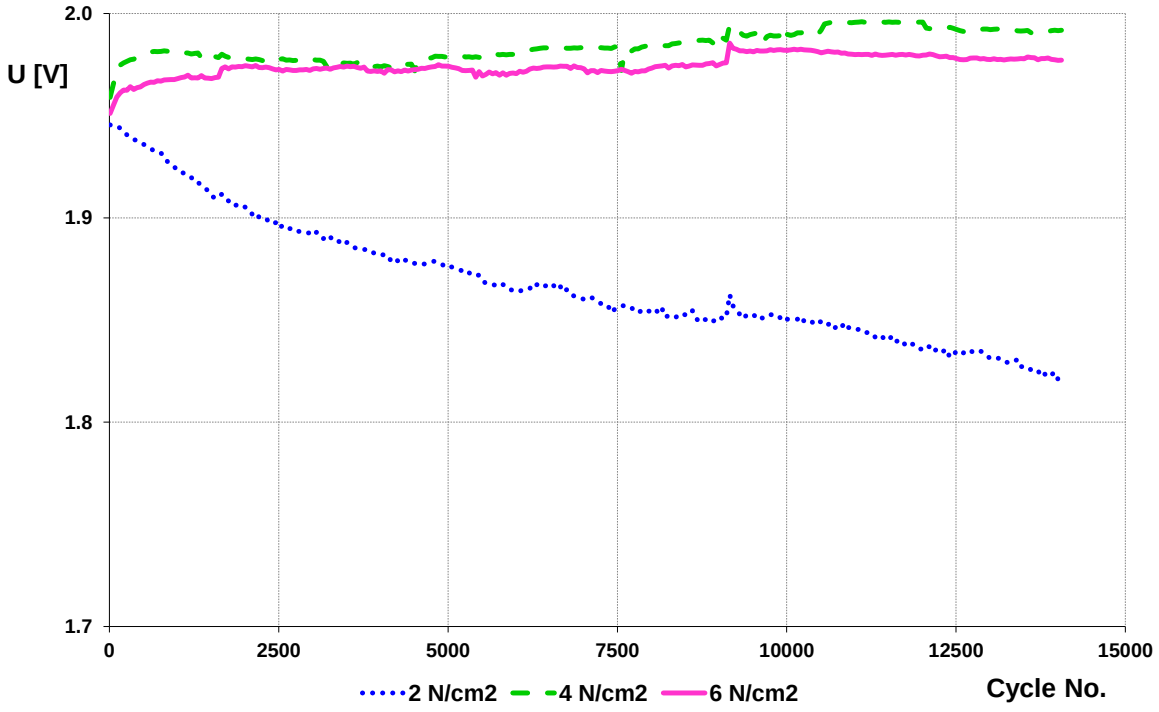


**Figure 8.** Dependence of cell voltage on discharging cycle number. Third PSoC run

*3.5. Final voltage and capacity*

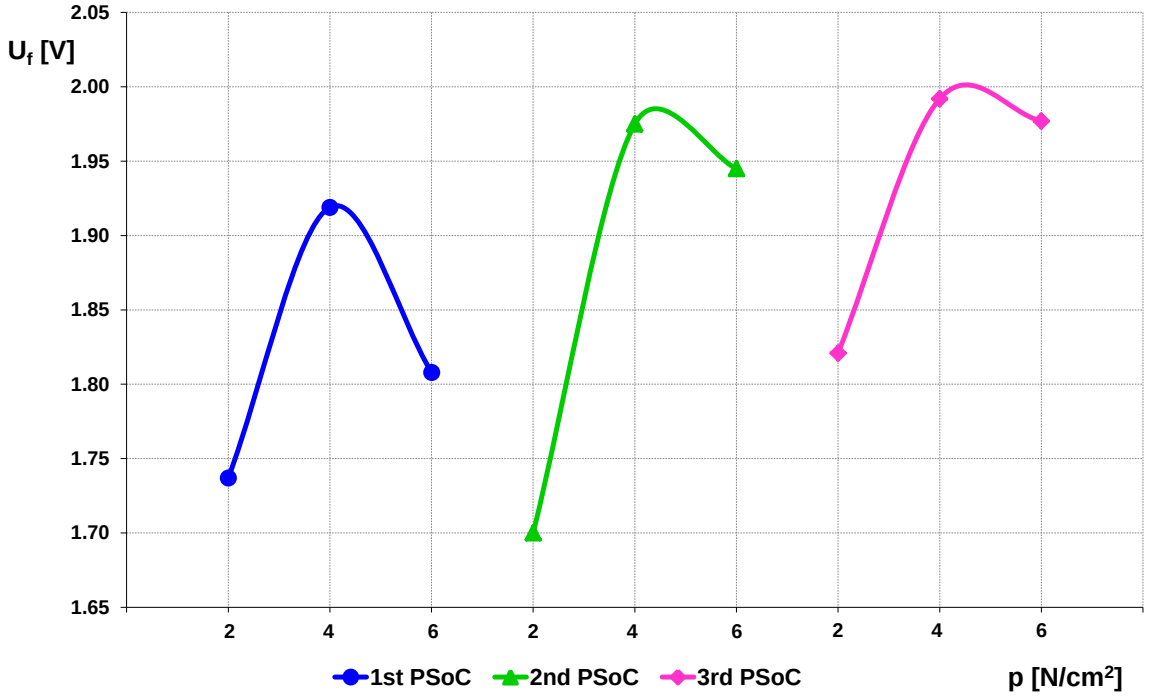


**Figure 9.** Dependence of the final voltage on the pressure in all PSoC runs

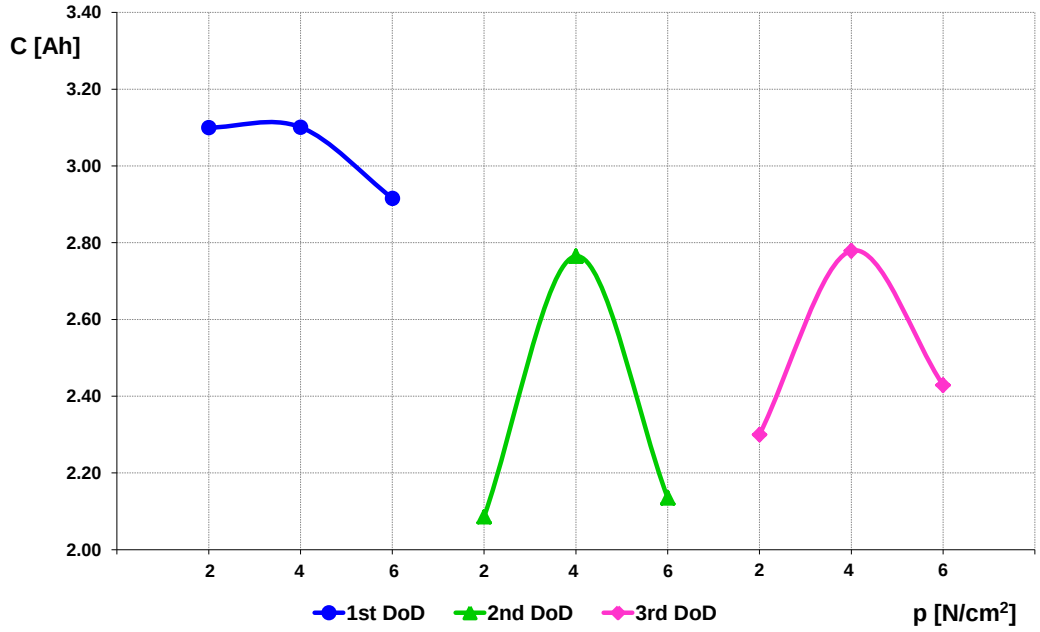


**Figure 10.** Dependence of the capacity voltage on the pressure in all DoD runs

A comparison final voltage at the end of all three runs of PSoC cycling that represents the cycle life of electrodes with various pressure is shown in Fig. 9. Hence, the most favourable pressure seems to be 4 $N.cm^{-2}$. This result corresponds to the result in the cited paper [7], where the most favorable pressure was found 4 $N.cm^{-2}$ at the electrodes with carbon and $TiO_2$ additives.

A comparison capacity at the end of all three runs of DoD cycling of electrodes with various pressure is shown in Fig. 10. Hence, the most favourable pressure seems to be again electrode with pressure 4 $N.cm^{-2}$ with the highest cycle life in all PSoC runs and the highest capacity in all DoD runs.

The worst is again electrode with the lowest compression, which has in all PSoC runs the smallest cycle life (lowest final voltage) and its capacity with the exception of the first DoD run is also the smallest in all DoD runs.

### *3.6. Contact resistance and active mass resistance.*

During all three PSoC runs it was measured contact resistance and active mass resistance of the negative electrodes using our original method [18].

The highest value of contact resistance and active mass resistance has the electrode with the lowest pressure. Both of these values during the first PSoC run grow to levels around 3 mΩ at the end of the first PSoC run.

High internal resistance is associated with poor charge acceptance during charging caused by low pressure of the negative active mass.

The lowest value of contact resistance and active mass resistance (approx 0.3 mΩ) achieves the cell with pressure of 4 $N.cm^{-2}$. This value preserves during all of PSoC runs. Optimal pressure seems to ensure low internal resistance and a sufficiently high porosity of negative active mass.

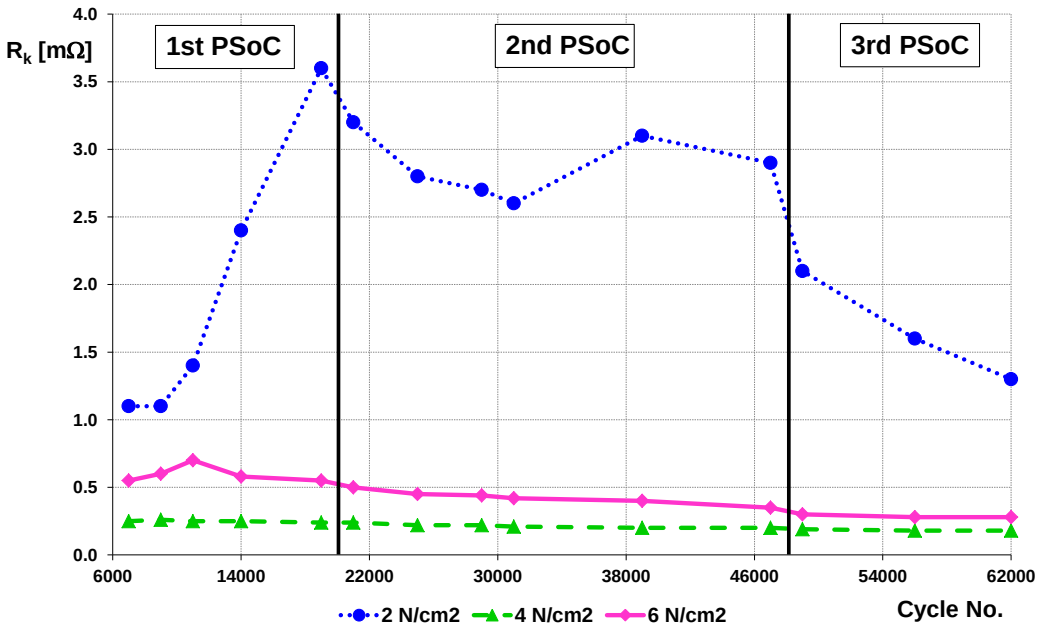


**Figure 11.** Schematic evolution of the contact resistance for the tested electrodes

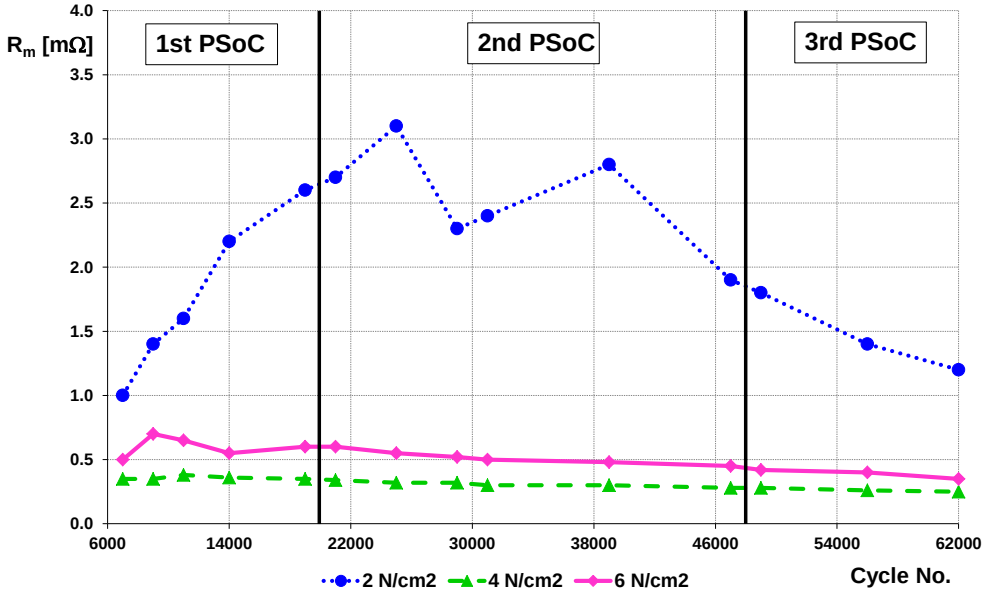


**Figure 12.** Schematic evolution of the active mass resistance for the tested electrodes

The cell with pressure of 6 N.cm$^{-2}$ has contact resistance and active mass resistance about 0.5 mΩ higher than cell with pressure of 4 N.cm$^{-2}$. During PSoC runs its value gradually decreases and approaches the value of the cell with optimum pressure 4 N.cm$^{-2}$.

In our preceding work with electrodes containing powdered carbon under mechanical pressure [16], where the cycle life of the experimental cells exceeded 100 thousand PSoC cycles, the highest active mass resistance reached the cell with the lowest pressure as in this work. The difference is in the size of the active mass resistance. For the cell with carbon additive and the lowest pressure of 2 N.cm$^{-2}$ it was only 0.5 mΩ, for cells with the highest pressure of 6 N.cm$^{-2}$ it was 0.2 mΩ. In this work, the resistance of the active mass for the cell containing glass fibres with the lowest pressure of 2 N.cm$^{-2}$ reaches values around 3 mΩ, which greatly affects cycle life in the PSoC cycling and also capacity in the DoD cycling.

## 4. CONCLUSIONS

Microscopic glass fibres in negative active mass of lead acid electrodes cause nearly the same effect as carbon or titanium dioxide in prolonging the cycle life during PSoC. This effect can be considerably accentuated by applying mechanical compression to the electrodes, preferably of the magnitude of 4 N.cm$^{-2}$.

From the resulting dependencies, we can conclude the least suitable seems to be the lowest pressure (2 N.cm$^{-2}$). Low pressure causes an increase in internal resistance and this can cause progressive expansion of the negative active mass. High internal resistance is associated with poor

charge acceptance during charging (reduction of charging efficiency), with a decrease in cycle life in the course of PSoC cycling and also with capacity decrease during DoD cycling.

The best pressure seems to be pressure around 4 $N.cm^{-2}$. Optimum pressure causes stabilization of negative active mass structure, reduction of internal resistance and a preservation of sufficiently high porosity of the negative active mass.

The higher pressure (6 $N.cm^{-2}$) causes a decrease of negative active mass and separator porosity (capacity reduction) and also increases the risk of short circuits during exploitation.

ACKNOWLEDGEMENTS
The glass fibres were kindly provided by Tony Ferreira, Hollingsworth&Vose Co., West Groton, MA, USA. This research work has been carried out in the Centre for Research and Utilization of Renewable Energy (CVVOZE). Authors gratefully acknowledge financial support from the Ministry of Education, Youth and Sports of the Czech Republic under NPU I programme (project No. LO1210)

**References**

1. B. Culpin, D.A.J. Rand, *J. Power Sources* 36 (1991) 415.
2. A. Cooper, P.T. Moseley, *J. Power Sources* 113 (2003) 200.
3. L.T. Lam, C.G. Phyland, D.A.J. Rand, A.J. Urban, ALABC Project No. C 2.0, Progress Report.
4. M. Calábek, K. Micka, P. Křivák, P. Bača, *J. Power Sources* 158 (2006) 864–867.
5. K. Nakamura, M. Shiomi, K. Takahashi, M. Tsubota, *J. Power Sources* 59 (1996) 153.
6. M. Shiomi, T. Funato, K. Nakamura, K. Takahashi, M. Tsubota, *J. Power Sources* 64 (1997) 147.
7. A.F. Hollenkamp, W.G.A. Baldsing, O.V. Lim, R.H. Newnham, D.A.J. Rand, J.M. Rosalie, D.G. Vella, L.H.Vu, ALABC Project No. N1.2, Annual Report, July 2000–June 2001.
8. F. Saez, B. Martinez, D. Marin, P. Spinelli, F. Trinidad, *J. Power Sources* 95 (2001) 174.
9. M. Calábek, K. Micka, P. Bača, P. Křivák, L. Šácha, ALABC Project No. AMC-10, Final Report.
10. K.J. Vetter, *Chem. Ing. Techn.* 45 (1973) 213.
11. N.A. Hampson, J.B. Lakeman, *J. Power Sources* 6 (1981) 101.
12. Z. Takehara, *J. Power Sources* 85 (2000) 29.
13. P. Ekdunge, D. Simonsson, in: K.R. Bullock, D. Pavlov (Eds.), Proceedings of Advances in Lead-Acid Batteries, The Electrochem. Soc., Inc., Pennington, NJ, 1984, p. 252.
14. A. Tokunaga, M. Tsubota, K. Yonezu, K. Ando, in: K.R. Bullock, D. Pavlov (Eds.), Proceedings of Advances in Lead-Acid Batteries, The Electrochem. Soc., Inc., Pennington, NJ, 1984, p. 314.
15. K. Micka, I. Roušar, *Electrochim. Acta* 21 (1976) 599.
16. P. Bača, K. Micka, P. Křivík, K. Tonar, P. Tošer, *J. Power Sources* 207 (2012) 37.
17. P. Bača, P. Křivík, P.Tošer, S. Vaculík, *Int. J. Electrochem. Sci.,* 10 (2015) 2206.
18. M. Calábek, K. Micka, P. Bača, P. Křivák, V. Šmarda, *J. Power Sources* 62 (1996) 161.
19. S. Zhu, J. Cheng, D. Zhu, G. Yang, *Int. J. Electrochem. Sci.* 8 (2013) 1928 – 1937.
20. A. Czerwiński, Z. Rogulski, S. Obrębowski, J. Lach, K. Wróbel1, J. Wróbel1, *Int. J. Electrochem. Sci.* 9 (2014) 4826 – 4839.